ELSEVIER

Coastal Engineering 42 (2001) 199–218

Coastal Engineering
An International Journal for Coastal, Harbour and Offshore Engineers

www.elsevier.com/locate/coastaleng

Establishing uniform longshore currents in a large-scale sediment transport facility

David G. Hamilton [a,*], Bruce A. Ebersole [b]

[a] *C5-310 Cain Ridge Road, Vicksburg, MS 39180, USA*
[b] *US Army Engineer Research and Development Center, Coastal and Hydraulics Laboratory, 3909 Halls Ferry Road, Vicksburg, MS 39180-6199, USA*

Received 30 November 1999; received in revised form 3 May 2000; accepted 27 September 2000

Abstract

A large-scale laboratory facility for conducting research on surf-zone sediment transport processes has been constructed at the U.S. Army Engineer Research and Development Center. Successful execution of sediment transport experiments, which attempt to replicate some of the important coastal processes found on long straight beaches, requires a method for establishing the proper longshore current. An active pumping and recirculation system comprised of 20 independent pumps and pipelines is used to control the cross-shore distribution of the mean longshore current. Pumping rates are adjusted in an iterative manner to converge toward the proper settings, based on measurements along the beach. Two recirculation criteria proposed by Visser [Coastal Eng. 15 (1991) 563] were also used, and they provided additional evidence that the proper total longshore flow rate in the surf zone was obtained. The success of the external recirculation system and its operational procedure, and the degree of longshore uniformity achieved along the beach, are the subjects of this paper. To evaluate the performance of the recirculation system, and as a precursor to sediment transport experiments, two comprehensive test series were conducted on a concrete beach with straight and parallel contours (1:30 slope), one using regular waves and the other using irregular waves. In the regular wave case, the wave period was 2.5 s and the average wave height at breaking was approximately 0.25 m. In the irregular wave case, the peak wave period was 2.5 s and the significant breaking wave height was approximately 0.21 m. The longshore current recirculation system proved to be very effective in establishing uniform mean longshore currents along the beach in both cases. This facility and the data presented here are unique for the following reasons: (1) the high cross-shore resolution of the recirculation system and the ease with which changes can be made to the longshore current distribution, (2) the degree of longshore uniformity achieved as a percentage of the length of the basin (even near the downdrift boundary), (3) the scale of the wave conditions generated, and (4) the relatively gentle beach slope used in the experiments (compared to previous laboratory studies of the longshore current). Measured data are provided in an appendix for use in theoretical studies and numerical model development and validation.

Keywords: Longshore currents; Surf zone currents; Wave and current measurements; Laboratory experiments; Large-scale laboratory facility

* Corresponding author. Tel.: +1-601-634-1597; fax: +1-601-634-4314.
E-mail address: cherylquillin@juno.com (D.G. Hamilton).

0378-3839/01/$ - see front matter
PII: S0378-3839(00)00059-4

Report Documentation Page

Form Approved
OMB No. 0704-0188

1. REPORT DATE	2. REPORT TYPE	3. DATES COVERED
2001		**00-00-2001 to 00-00-2001**

4. TITLE AND SUBTITLE	5a. CONTRACT NUMBER
Establishing uniform longshore currents in a large-scale sediment transport facility	5b. GRANT NUMBER
	5c. PROGRAM ELEMENT NUMBER
6. AUTHOR(S)	5d. PROJECT NUMBER
	5e. TASK NUMBER
	5f. WORK UNIT NUMBER
7. PERFORMING ORGANIZATION NAME(S) AND ADDRESS(ES) **Army Engineer Research and Development Center,Coastal and Hydraulics Laboratory,3909 Halls Ferry Road,Vicksburg,MS,39180**	8. PERFORMING ORGANIZATION REPORT NUMBER
9. SPONSORING/MONITORING AGENCY NAME(S) AND ADDRESS(ES)	10. SPONSOR/MONITOR'S ACRONYM(S)
	11. SPONSOR/MONITOR'S REPORT NUMBER(S)

12. DISTRIBUTION/AVAILABILITY STATEMENT
Approved for public release; distribution unlimited

13. SUPPLEMENTARY NOTES

14. ABSTRACT

15. SUBJECT TERMS

16. SECURITY CLASSIFICATION OF:			17. LIMITATION OF ABSTRACT	18. NUMBER OF PAGES	19a. NAME OF RESPONSIBLE PERSON
a. REPORT **unclassified**	b. ABSTRACT **unclassified**	c. THIS PAGE **unclassified**		**20**	

1. Introduction

Waves breaking at oblique angles to the coastline generate a mean current in the surf zone that flows parallel to the coast. Breaking waves and the longshore current are capable of transporting hundreds of thousands of cubic meters of sand along the coastline during a typical year. One motivation for studying the longshore current and longshore sand transport is to improve existing methods for calculating nearshore sediment transport rates, which can then be applied to practical engineering applications such as: predicting beach response in the vicinity of coastal structures, beach-fill project evolution and renourishment requirements, and sedimentation rates in navigation channels.

The Large-scale Sediment Transport Facility (LSTF) has been constructed at the U.S. Army Engineer Research and Development Center's Coastal and Hydraulics Laboratory (see Rosati et al. 1995). The intent for the facility is to reproduce, in a finite-length wave basin, certain surf zone processes found on a long straight natural beach, including sand transport and beach change processes. Successful execution of sediment transport experiments requires a method for establishing the proper longshore current, or at least a reasonable representation of the proper longshore current recognizing that all processes that occur on real beaches are not simulated in the facility. In the context of this paper, the term "proper" longshore current is used to describe the longshore current that would be generated along an infinitely long beach having a cross-section and incident wave forcing that are invariant in the longshore direction. An active pumping and re-circulation system is used in the LSTF to establish the proper longshore current (see Hamilton et al. 1996, 1997).

As a design objective, the external recirculation system and procedures for operating it should maximize the length of beach for which waves, currents, sediment transport, and beach morphology are nearly uniform in the alongshore direction. Longshore uniformity is important both in regions where wave, current, and sediment concentration measurements are made and at the downdrift boundary of the beach where sand traps are located. Creating the proper longshore current and a high degree of longshore uniformity are difficult to achieve. The capability of the LSTF recirculation system to meet these objectives is the subject of this paper. Two comprehensive series of longshore current experiments were performed on a fixed concrete beach to facilitate evaluation of the system. The experiments were done as a precursor to a more complex series of moveable-bed longshore sediment transport experiments.

The paper is organized as follows. Section 2 provides a brief overview of previous laboratory investigations of longshore currents, with emphasis on the method used to create the proper longshore current. Section 3 provides a brief description of the layout of the LSTF, as well as the design of the external recirculation system and the lateral boundaries. Section 4 gives an overview of the experimental program along with the incident wave conditions generated for both test series. Section 5 describes the methodology used to acquire data, and the type of data collected during each experiment. Section 6 describes the procedure used to establish the proper longshore currents. Section 7 quantifies the longshore uniformity of the waves, currents and mean water surface elevation, as a function of beach length. Section 8 discusses the steadiness of the flow rates in the basin and the repeatability of the flow measurements. Section 9 discusses the results from the standpoint of conducting longshore sediment transport experiments in the LSTF in the near future. Section 10 provides conclusions.

2. Previous laboratory investigations of longshore currents

Relatively few carefully controlled laboratory studies, which involved the study of longshore currents, have been conducted. In the earliest investigations, only the average longshore current velocity, across the width of the surf zone, or the maximum velocity, was measured (Putnam et al., 1949; Brebner and Kamphuis, 1963). Galvin and Eagleson (1965) were the first to measure the cross-shore distribution of the longshore current at several shore-normal transects along the beach. This increased detail, although very valuable, revealed some of the challenges associated with obtaining longshore uniformity in the laboratory. All three of these stud-

ies used passive recirculation systems, which means that the longshore current was allowed to passively flow back to the upstream end of the basin, either inside or outside of the waveguides.

Dalrymple and Dean (1972) developed a circular wave basin with a spiral wave generator and a circumferential beach to eliminate the boundary effects caused by the upstream and downstream boundaries of the facility. Potential methods to deal with the problem of wave-induced circulation in shallow wave basins continued to be addressed in subsequent years, see Dalrymple et al. (1977) and Kamphuis (1977).

Visser (1980, 1982, 1984, 1991) documented the most comprehensive laboratory study of longshore currents previously conducted for a relatively wide range of test conditions. Visser measured the three-dimensional structure of the longshore current and developed a method to maximize longshore uniformity by utilizing an active external recirculation system driven by a pump. A distribution system was used at the upstream boundary to distribute the longshore flux across the surf zone. At the downstream boundary, however, a distribution system was not used, but the width of the opening in the waveguide was optimized based on the width of the surf zone. The longshore current then flowed further downstream toward a single point of intake to the external recirculation system. This laboratory study sets a high standard for experimental design and attention to detail. The experiments were conducted on relatively steep beach slopes (1:10 and 1:20) and were restricted to longshore currents generated by regular waves.

Reniers and Battjes (1997) measured the cross-shore distribution of longshore current for regular and irregular waves, and they used a similar method of external recirculation as that used by Visser. Tests where conducted on two types of beaches; one with a constant 1:20 beach slope and one with an offshore bar. In the case of the barred beach, measurements revealed a bimodal longshore current distribution with one peak near the crest of the offshore bar and the second peak near the shoreline. For the case of the constant beach slope, the limited geometric scale of the experiments made it impossible to measure the peak longshore current, due to inadequate water depth in the surf zone.

Mizuguchi and Horikawa (1978) were the first to measure the vertical structure of the longshore current in the laboratory. A passive recirculation scheme was used allowing the longshore current to recirculate outside of the downstream waveguide and re-enter into the testing region beneath the wave generators. They found the mean longshore current to be relatively uniform with depth. Visser (1991) observed the same. Simons et al. (1995) concluded that the vertical velocity structure of the longshore current followed a logarithmic profile during preliminary evaluation tests in the large-scale Coastal Research Facility at HR Wallingford. The active recirculation system used in the Coastal Research Facility is a further improvement upon the system used by Visser (1991) in that adjustable weirs are used to control the cross-shore distribution of longshore current at both the upstream and downstream boundaries of the facility (HR Wallingford, 1994). Hamilton et al. (1997) summarizes the seven types of longshore current recirculation systems used in laboratory investigations of longshore currents.

3. Design of the LSTF

Fig. 1 is a photograph of the LSTF taken during a regular wave experiment. The LSTF has dimensions of approximately 30-m cross-shore by 50-m longshore by 1.4-m deep, see Fig. 2. Unidirectional, long-crested waves are generated with four piston-type wave generators. The concrete beach has a longshore dimension of 31 m and a cross-shore dimension of 21 m, with a plane slope of 1:30. Small longshore variations in beach elevation can have a significant influence on longshore current patterns (Putrevu et al., 1995). Therefore, the beach was designed and carefully constructed with straight and parallel contours and a high degree of accuracy (vertical variation of ± 2 mm).

The coordinate system in the facility is right-handed, with the origin at the downstream, shoreward end of the wave basin (see Fig. 2). The positive x-axis is directed offshore and is measured relative to the upper edge of the concrete beach slope. The positive y-axis is directed upstream. The z-axis is measured positively upwards with the origin at the still water level. The coordinate system was chosen

Fig. 1. Oblique view of the Large-scale Sediment Transport Facility (regular wave experiment). A technician standing in the upper left corner indicates the physical size of the facility.

based on future plans to extend the length of the wave basin. However, for the sake of simplicity, all downstream-directed longshore current speeds and flow rates presented in the paper are given as positive numbers, even though the flow is in the negative y direction.

The external recirculation system consists of 20 independent pump-and-piping systems with a total capacity of 1250 l/s. Hamilton et al. (1996) describe the methodology used to determine the capacity and functional requirements of this system. Twenty flow channels at the downstream end of the facility guide the longshore current from the beach to the pumps (see Fig. 2). Likewise, on the upstream end, 20 flow channels guide the flow from the point of pipe discharge to the upstream boundary of the beach. Flow channels extend from $x = 3.0$ to 18.0 m in the cross-shore direction, and each channel is 0.75 m wide. This design allows a large range of longshore current magnitudes and cross-shore distributions to be accurately controlled and externally recirculated. Hamilton et al. (1997) provides design details for each of the primary components in the recirculation system.

Design of the upstream and downstream lateral boundaries was a challenge since the longshore current has to flow out of and into the flow channels while wave diffraction into the flow channels needs to be minimized. Waveguides were designed so that the height of the opening beneath the waveguide could be adjusted to allow the longshore current to pass beneath the impermeable waveguide. For the wave conditions and water level used during these experiments, the height of the opening was selected after several trial and error iterations. At the upstream boundary a constant 0.1-m high opening be-

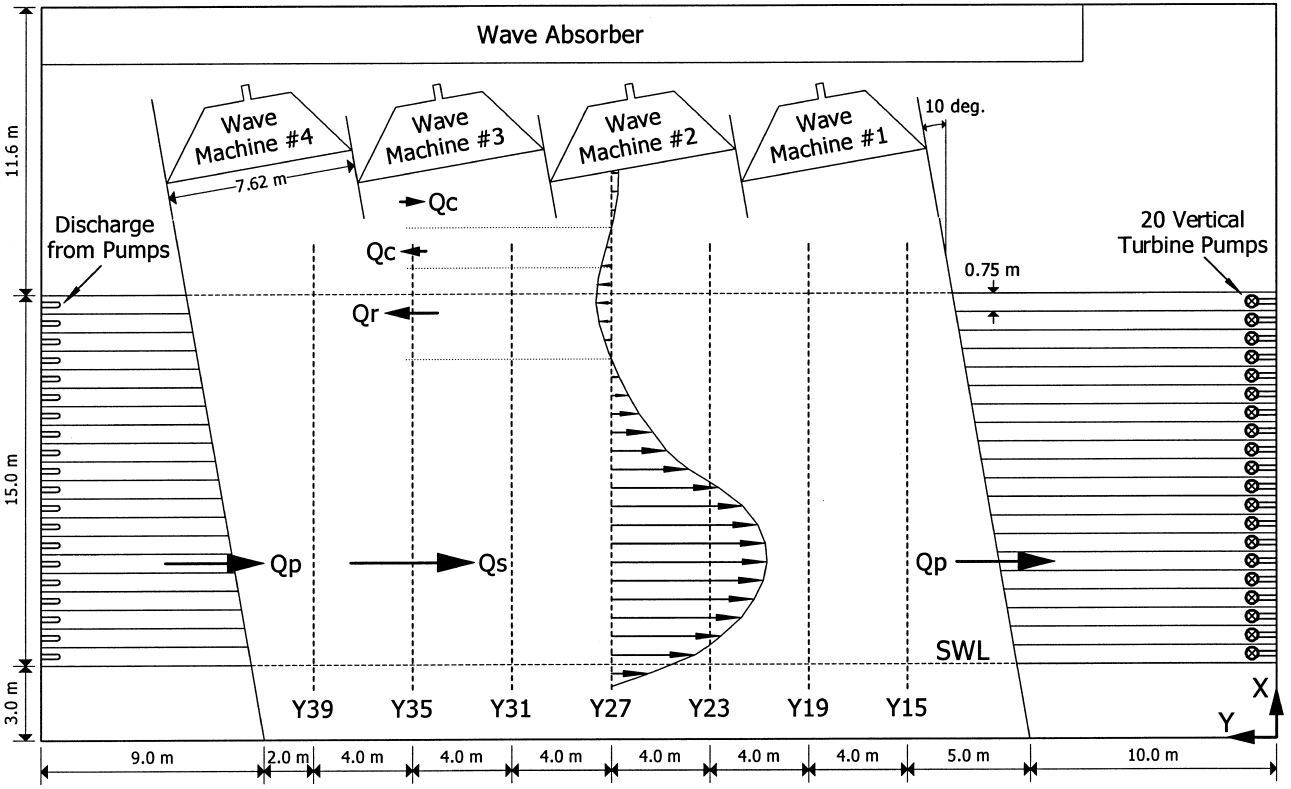

Fig. 2. Plan view of the LSTF and a conceptual diagram of longshore flow conditions.

neath the waveguide was used. At the downstream boundary, the bottom edge of the waveguide was set at approximately the minimum wave trough elevation. In addition to the waveguides, a matrix of 0.1-m diameter rigid polyvinyl chloride pipe was installed in each of the flow channels to absorb the residual wave energy that entered beneath the waveguides, and to minimize wave reflection in the flow channels. Svendsen (1991) discussed similar concepts. Additional information regarding the design and evaluation of the performance of the LSTF is documented in Hamilton et al. (2000).

4. Experimental program

A number of preliminary experiments were conducted to investigate: (a) long-term oscillations in pump discharge rates (they were found to be negligible), (b) flow patterns created by pumping only (i.e., no wave forcing), (c) flow patterns with waves only (i.e., no external current recirculation), and (d) the time required for the mean velocities in the wave basin to reach steady state.

Once these preliminary experiments were completed, two comprehensive test series were conducted, one using regular waves and the other using irregular waves. A total of 20 experiments were conducted, each with a different magnitude and cross-shore distribution of pumped flow rate. Fifteen regular wave experiments were conducted in the process of determining the proper magnitude and cross-shore distribution of the longshore current, and were identified as Test 2 (waves only) and Tests 6A–N (waves and currents). Five irregular wave experiments were conducted and identified as Tests 8A–E.

The incident wave conditions adopted for Tests 6A–N and Tests 8A–E are given in Table 1 where T is the wave period (peak spectral wave period, T_p, for the irregular wave case), H is the wave height (energy-based significant wave height, H_{mo}, for the irregular wave case), λ is wavelength, d is still water depth, θ is the angle of incidence relative to shore normal, and the subscripts "0" and "1" refer to values in deep water and at the wave generators, respectively. Deepwater values were calculated using linear wave theory. For the irregular wave tests, H_{mo} was selected so that the root-mean-square wave height, H_{rms}, was comparable to the average wave height, H_{avg}, for the regular wave case. Therefore, the total incident wave energy used for both regular and irregular waves was similar. For the irregular wave tests, a TMA spectrum was used to define the spectral shape. The spectral width parameter was 3.3, a value representing typical wind sea conditions. A random phase method was used to synthesize the pseudo-random wave train used to drive the wave generators. The length of the drive signal was 500 s, a duration of 200 times the peak wave period (2.5 s). The still water depth at the wave generators was held constant at 0.667 m during all experiments.

5. Measurement methodology

An automated instrumentation bridge was used to position the wave and current sensors at various positions along the beach. Transect locations were selected every 4.0 m, from $y = 15.0$ to $y = 39.0$ m, as shown in Fig. 2. Transects are identified as Y15, Y19, Y23, Y27, Y31, Y35 and Y39, according to their longshore coordinate. During each experiment, measurements were made along at least three primary transects to represent general hydrodynamic conditions along the beach: Y19 (center of the downstream half of the beach), Y27 (center of the entire

Table 1
Summary of incident wave conditions

Test	Wave type	T (s)	H_1 (m)	H_1/λ_1 (–)	d_1 (m)	θ_1 (°)	H_0 (m)	H_0/λ_0 (–)	θ_0 (°)
Test 6A–N	Regular	2.5	0.182	0.031	0.667	10.0	0.189	0.019	16.6
Test 8A–E	Irregular	2.5	0.225	0.038	0.667	10.0	0.233	0.024	16.6

beach), and Y35 (center of the upstream half of the beach). During Tests 6N and 8E, and several others, measurements were made at all seven transects.

Ten capacitance-type wave gauges and 10 acoustic-doppler velocitimeters (ADV) were co-located in a cross-shore array on the instrumentation bridge. Wave and current sensors are numbered in ascending order, starting with number 1 and moving offshore to number 10. Four other wave gauges were fixed in an array along the $x = 18$ m contour line, one centered in front of each wave generator. Wave set-up and set-down were obtained by using the wave gauges to measure the elevation of the still water level prior to each experiment and then subtracting that elevation from the mean water surface elevation measured during the experiment. The ADV's were set at elevations approximately one third of the water depth above the bed.

At the beginning of each experiment, the instrumentation bridge was positioned at Y27 and the elevation of the still water level was measured with all 14 wave gauges. Then the pumps were turned on and set to prescribed discharges (see Section 6) to create the desired longshore current distribution. Data collected with the in-line flow sensors (one in each of the 20 pump-and-piping systems) were analyzed to ensure the pumps were operating at the proper flow rates. The wave generators were then turned on and run continuously throughout the experiment. After 10 min of wave generation (20 min since the time the pumps were started) data collection began at the Y27 transect. All sensors were sampled at 20 Hz for 500 s during both the regular and irregular wave test series. The process of repositioning the instrumentation bridge and acquiring 500 s of data was repeated at transects Y15, Y19, Y23, Y27, Y31, Y35, and Y39. After the last transect was completed at Y39, a third set of data was acquired at Y27. Redundant measurements at transect Y27 were collected to assess repeatability of the measurements and the steadiness of the hydrodynamic conditions (see results in Section 8).

The time series were visually inspected while the experiments were conducted to assess data quality. In very shallow water (ADV 1 and 2), air bubbles from breaking waves penetrated into the water column, to the depth of the ADV sensors, causing undesirable spikes in the velocity time series. These spikes were removed during post-processing with a filtering routine developed specifically to handle the characteristics of the spikes. The ADV measurements further offshore did not need to be filtered.

Detailed dye measurements were performed during each experiment to inspect patterns in the flow streamlines by injecting dye into the water at discrete points. Dye observations focused on: (a) straightness of the flow streamlines along the beach, (b) streamline patterns of flow exiting the upstream flow channels and approaching the downstream flow channels, and (c) streamlines in the offshore region of the basin where internal recirculation occurred. Dye was also used to obtain qualitative information on the longshore current in very shallow water, shoreward of ADV 1.

6. Procedure for tuning the longshore current

Section 6.1 describes the iterative process that was used to establish the proper magnitude and cross-shore distribution of the longshore current along the beach by adjusting the pump settings for the external recirculation system. To verify these results, Sections 6.2 and 6.3 describe two criteria proposed by Visser to confirm that the proper total longshore flow rate was being recirculated. However, these two criteria consider only the magnitude of the total longshore flow rate. They do not help determine the proper cross-shore distribution of the longshore current that needs to be recirculated.

Fig. 2 illustrates conceptually the flow conditions in the LSTF during the experiments. The quantity Q_s is the total longshore flow rate in the surf zone between the wave set-up limit and the point of transition where the mean longshore current reverses direction; Q_p is the total longshore flow rate actively pumped through the external recirculation system; Q_r is the total longshore flow rate that internally recirculates in the offshore region; and Q_c is a secondary offshore circulation cell limited to the length of each wave board, between two adjacent baffles. In this facility, Q_c develops as a result of the baffles that extend shoreward of the wave boards. In general, it was found that Q_c decreases as Q_r decreases, because Q_r drives Q_c. At a transect midway along the

beach, and assuming no temporal change in mean water level within the wave basin,

$$Q_s = Q_p + Q_r \quad (1)$$

6.1. Iterative examination of the longshore current distribution

Pump settings were systematically adjusted in an effort to establish the proper mean longshore current distribution in the surf zone, for a given wave condition. As the series of experiments progressed, new estimates of the proper longshore current distribution were made based on previously measured distributions along the beach. The following hypotheses were used to guide the tuning process: (1) the degree of uniformity of longshore current in the surf zone should increase as the proper longshore current distribution is approached; (2) the magnitude of internal recirculation, Q_r, should decrease as the proper longshore current distribution is approached; (3) there is a point where Q_r is minimized, and (4) internal recirculation cannot be completely eliminated due to imperfections of the lateral boundaries.

The first regular wave experiment, Test 2, was conducted with no pumping ($Q_p = 0$ l/s). This test was conducted to investigate the case when Q_r had the largest magnitude and to examine the signs of under-pumping. This test is equivalent to the recirculation scheme used by Putnam et al. (1949), and discussed by Visser (1991) and Hamilton et al. (1997). As expected, results from Test 2 showed very non-uniform conditions both in the magnitude and distribution of longshore current measured at Y19, Y27, and Y35.

A total of 14 regular wave experiments were conducted with $Q_p > 0$ l/s. An initial estimate of the proper longshore current distribution was made using the numerical model NMLONG (Kraus and Larson, 1991). The breaking wave height-to-depth ratio, used as a calibration parameter in the numerical model, was adjusted based on wave height measurements made in the laboratory experiments.

Fig. 3 shows pump settings for seven of the 14 experiments, including what turned out to be the proper distribution, Test 6N, for comparison. Pump settings are shown in terms of the depth-averaged longshore current pumped through the lateral boundaries of the facility. As illustrated, the proper longshore current distribution was approached initially by under-pumping across the entire surf zone, and then gradually increasing the flow rate pumped through the lateral boundaries.

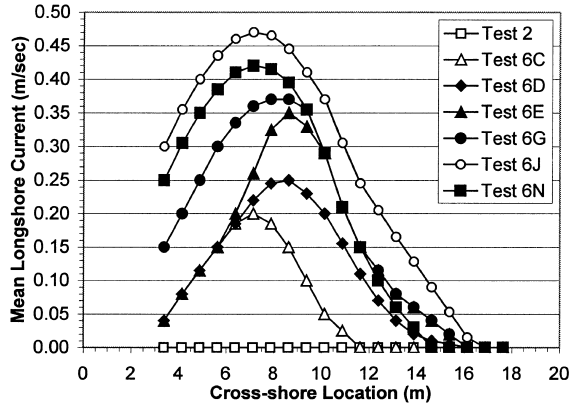

Fig. 3. Progression of pump settings for regular wave tests.

Results from Test 6D, an under-pumped case that was the fifth experiment in the series, are shown in Fig. 4. The peak longshore current measured at each of the three transects was much higher than the peak current pumped through the lateral boundaries. Offshore recirculation was diminished substantially in both extent and magnitude, compared to the no-pumping case; however, recirculation remained rather strong at Y27. The longshore current distribution at Y35 showed a region of flow reversal near the shoreline (negative values). This phenomenon was observed during all 15 experiments, and was found to be limited within a region extending from the upstream boundary to $y = 34$ m and offshore 2 m from the still-water shoreline. This region of flow reversal decreased significantly in magnitude and spatial extent as the proper distribution was approached with subsequent pump settings, but it was never completely eliminated.

By the tenth experiment (Test 6I) it appeared that the proper longshore current distribution was being approached at the peak and shoreward of the peak. However, there was concern that the offshore tail of the distribution was being over-pumped. To investigate the ramifications and signs of over-pumping, Test 6J was performed. Fig. 3 shows the longshore current distribution that was recirculated in Test 6J,

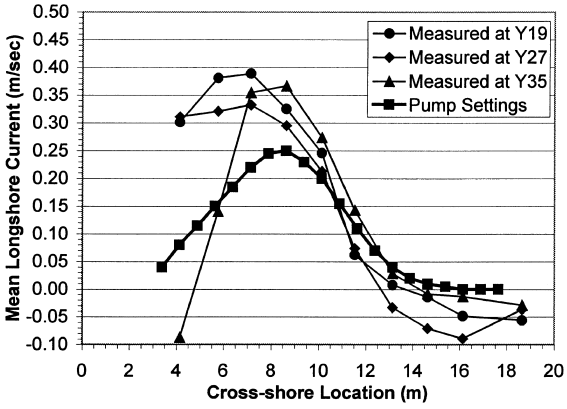

Fig. 4. Test 6D: under pumping at lateral boundaries.

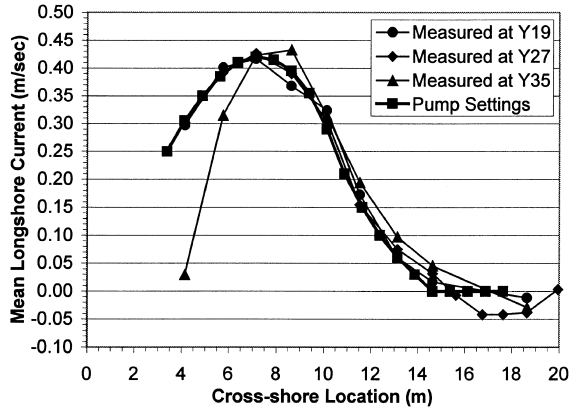

Fig. 6. Test 6N: proper pumping at lateral boundaries.

relative to other tests, and Fig. 5 shows longshore current results from the test. In the surf zone, the measured current distribution matched the pump settings quite well. In this region, it would be difficult to discern whether or not the lateral boundaries were being over-pumped. However, the over-pumped case (Test 6J) produced substantially more recirculation in the offshore region, relative to Test 6I. The results from this experiment indicated that there are signs of over pumping, but the results are subtle and not obvious over much of the longshore current distribution, except in the offshore tail.

The last few experiments (6K through 6N) focused in more detail on the offshore tail of the distribution, which proved to be more difficult to tune. Fig. 6 shows the results from Test 6N, the fifteenth and final iteration. Peak currents at the three primary transects were relatively uniform, and the degree of uniformity along much of the beach increased noticeably. In the offshore tail, agreement between pump settings and measurements was the best observed in any prior experiment. Current measurements in the offshore tail were always slightly greater than the pump settings, due to the internal recirculation. The magnitude and extent of the small flow reversal region near the shoreline at the upstream end of the beach was significantly less, and the longshore current measured closest to the shoreline at Y35 was now directed downstream (positive values). However, the flow reversal near the shoreline was still present further upstream. The flow reversal seemed to cause the higher current magnitude measured immediately offshore of the peak at Y35. The internal recirculation, Q_r was the lowest that had been observed during all previous tests, based on the measurements at the ADV furthest offshore. Therefore, it was concluded that the pump settings used during Test 6N were the proper settings, and they produced the highest degree of uniformity of longshore currents in the surf zone. Additional measurements were made offshore at the Y27 transect, to more accurately quantify the magnitude of the internal recirculation in the offshore region. They are discussed in more detail in the next section.

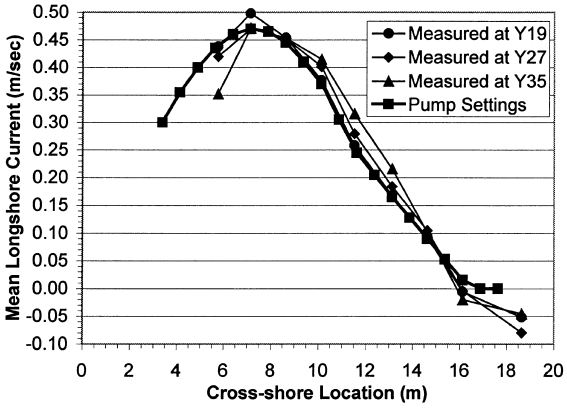

Fig. 5. Test 6J: over pumping at lateral boundaries.

The same iterative process used for the regular wave case was repeated for the irregular wave case. The final longshore current distribution was achieved in Test 8E, after five iterations. A more complete set

of results that illustrates the degree of longshore uniformity that was achieved, are presented and discussed later in Section 7 and provided in tabular form in Appendix A.

6.2. Verification using minimum Q_r concept

The values of Q_p used during Tests 6N and 8E, assumed to be the optimum values, were verified using the two criteria proposed by Visser (1991). As mentioned previously, these two criteria consider only the total longshore flow rate being recirculated, Q_p, not the cross-shore distribution (i.e., not the 20 individual pump flow rates).

In the present experiments, Q_r, which is influenced by Q_c (see Fig. 2), was estimated directly during Tests 6N and 8E, by making additional measurements in the offshore region at transect Y27. For all other experiments in the Tests 6 and 8 series, Q_r was estimated indirectly assuming $Q_r = Q_s - Q_p$ (Eq. (1)). Quantifying the magnitude of Q_c was difficult and it could only be roughly estimated using dye.

As shown in Appendix B, the mean longshore currents were rather invariant with depth. Therefore, the flow rate in the surf zone, Q_s, could be calculated using the longshore current measured one-third of the water depth above the bottom, the local mean water surface elevation, and an estimate of the cross-sectional area represented by each ADV. The pumped flow rate, Q_p, was calculated using data from the in-line flow sensors in each pump-and-piping system.

The first criterion proposed by Visser (1991) will be illustrated conceptually, using the Q_s and Q_r values obtained during the 15 regular wave experiments, see Fig. 7. Q_{pu} is the value of Q_p associated with the proper and nearly uniform longshore flow rate in the surf zone, Q_{su}. This method is based on the premise that Q_{pu} can be determined by minimizing Q_r as a function of Q_p. Visser (1991) postulated the following: (a) if $Q_p < Q_{pu}$, then the flow rate Q_s will increase in the downstream direction and the surplus, $Q_s - Q_p$, will return offshore and increase Q_r, or (b) if $Q_p > Q_{pu}$, then the increased flow rate Q_s will increase Q_r offshore due to increased advection and lateral friction.

Although there is some scatter in the data, Test 6N had the lowest value of Q_r. For Test 6N, Q_s and

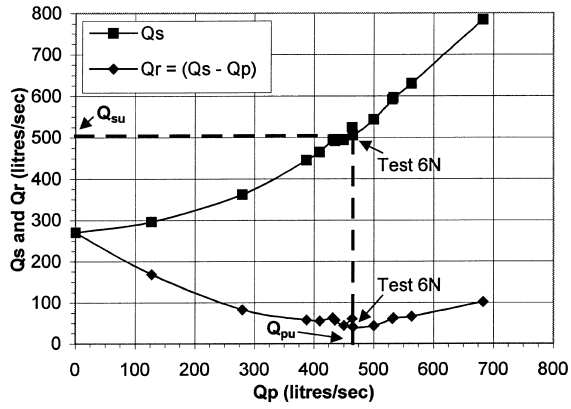

Fig. 7. Q_s and Q_r at Y27 for 15 regular wave experiments.

Q_p were 505 and 465 l/s, respectively. Hence, Q_r is indirectly estimated to be 40 l/s. Based on ADV measurements, the internal recirculation flowing in the upstream direction, $Q_r + Q_c$, was calculated to be 48 l/s. The secondary circulation cell, Q_c, flowing downstream directly in front of each wave generator was estimated to be 10 l/s, using dye. Therefore, the inferred value of Q_r was 38 l/s. Hence, direct measurement of the internal recirculation, Q_r, and the indirect estimate, $Q_s - Q_p$, gave good agreement. The ability to minimize internal recirculation relative to the flow rate in the surf zone, can be quantified as $(Q_s - Q_p)/Q_s$, which for this test was approximately 8%.

Values of Q_s and Q_r for the five irregular wave experiments are shown in Fig. 8. The slight upward curvature in the Q_r curve is evidence that Q_p had been increased sufficiently to reach the minimum value of Q_r, perhaps even slightly exceeding the proper flow rate, Q_{pu}, in Test 8E (the largest value of Q_p). However, evidence provided in the next section suggests that Q_p may have been slightly less than Q_{pu}. For Test 8E, Q_s and Q_p were calculated to be 545 and 478 l/s, respectively. Hence, Q_r is indirectly estimated to be 67 l/s. Based on ADV measurements $Q_r + Q_c$ was calculated to be 135 l/s. Based on dye measurements Q_c was estimated to be 60–70 l/s, flowing downstream directly in front of each wave generator. Therefore, the inferred value of Q_r was 65–75 l/s, and the value of Q_r and Q_c are comparable. Hence, both the direct and indirect measurements of the internal recirculation, Q_r, were in

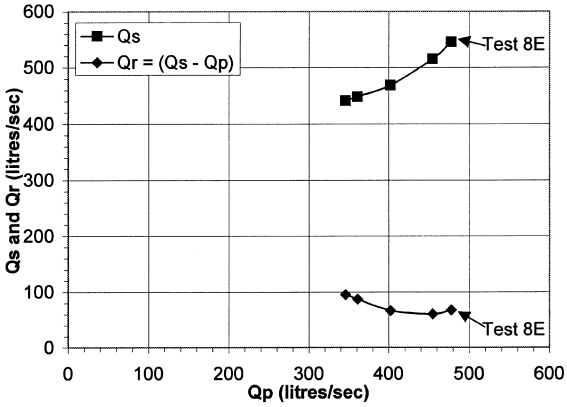

Fig. 8. Q_s and Q_r at Y27 for five irregular wave experiments.

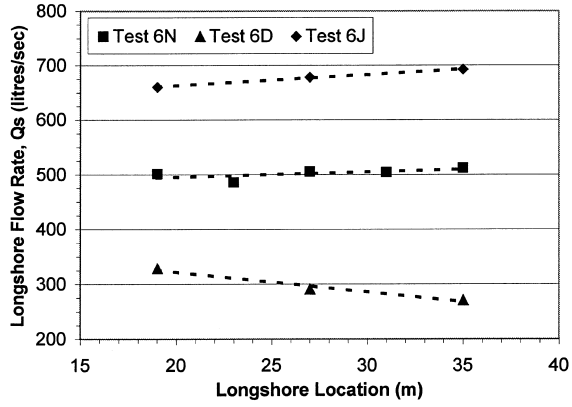

Fig. 9. Regular wave test series: longshore variation in Q_s.

relatively good agreement. For Test 8E the ratio of $(Q_s - Q_p)/Q_s$ was approximately 12%. More internal recirculation was generated in the irregular wave case because 2–3% of the waves broke slightly offshore of $x = 18$ m, the offshore limit of the external recirculation system.

Results for both the regular and irregular wave test series suggest that the recirculation criteria proposed by Visser (1991) is valid for the LSTF. However, for the LSTF, the gradient in the $Q_s - Q_p$ curve tends to increase more gradually as Q_p is increased, compared with the results presented by Visser (1991). Figs. 7 and 8 both suggest that Q_p could vary by as much as $\pm 20\%$, relative to Q_{pu}, without a significant increase in Q_r.

6.3. Verification using gradient in Q_s concept

The second method proposed by Visser (1991) is based on the following hypotheses: (a) if $Q_p < Q_{pu}$, then Q_s increases in the downstream direction, (b) if $Q_p = Q_{pu}$, then Q_s is essentially uniform in the longshore direction, and (c) if $Q_p > Q_{pu}$, then Q_s decreases in the downstream direction.

Fig. 9 shows results from three of the 15 regular wave experiments. In Test 6D, Q_p was approximately 40% less than the value of Q_p in Test 6N (the proper value), and Q_s increases in the downstream direction. Conversely, in Test 6J, Q_p was approximately 47% larger than Q_p in Test 6N and, as shown, Q_s decreases in the downstream direction. In Test 6N, Q_s is essentially uniform in the alongshore direction. These results give credence to the conclusion made previously that Test 6N represents the proper longshore current distribution for the regular wave case. However, in the case of under- or over-pumping, the longshore gradient in Q_s is relatively small. Therefore, significant care needs to be taken during the iterative process of selecting and converging on the proper longshore current distribution.

Results from two of the five irregular wave experiments are shown in Fig. 10. In Test 8A, Q_p was approximately 28% less than the value of Q_p in Test 8E, and Q_s increases in the downstream direction. Results for Test 8E (judged to be the proper value of Q_p) show that Q_s increases slightly in the downstream direction, which suggests that Q_p may have

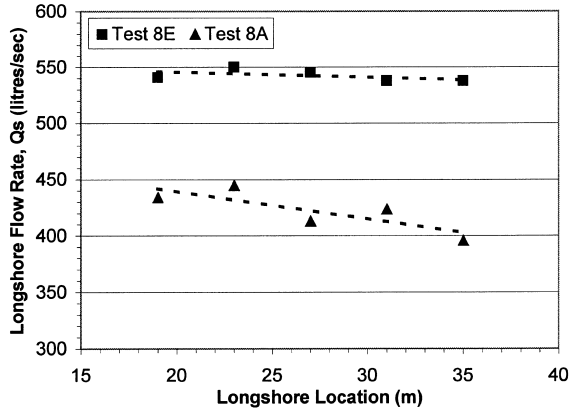

Fig. 10. Irregular wave test series: longshore variation in Q_s.

been slightly smaller than Q_{pu}. However, this contradicts evidence shown previously in Fig. 8 that suggested that Q_p was slightly larger than Q_{pu}. This slight discrepancy between the two methods may be caused by the fact that, in the LSTF, Q_p can vary by as much as $\pm 20\%$ of Q_{pu} without a significant increase in Q_r, as mentioned previously. Therefore, it was concluded that Q_p in Test 8E was essentially the proper longshore current distribution for the irregular wave test series. A case involving significant over-pumping was not conducted for the irregular wave experiments.

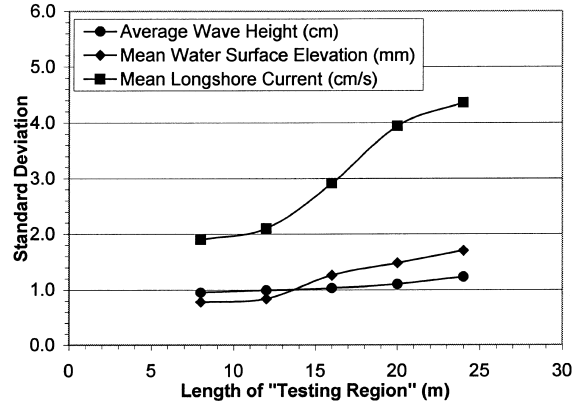

Fig. 11. Test 6N: longshore uniformity of hydrodynamics.

7. Longshore uniformity

This section quantifies the length of surf zone with the highest degree of longshore uniformity of the hydrodynamic processes. In general, it can be assumed that longshore uniformity should increase with increasing distance from the lateral boundaries. However, from the perspective of measuring longshore sediment transport in the LSTF, it is important to quantify the spatial limits of this region; especially at the downstream end where sand traps will be located.

Longshore uniformity was quantified by an average value of the standard deviation at each cross-shore position, and at each transect within the length of surf zone being evaluated. For both Test 6N and Test 8E, the standard deviation was calculated independently for the wave height, mean water surface elevation, and mean longshore current data sets. A new value of the average standard deviation was calculated each time the representative beach length was decreased, by excluding data from one or more transects from the calculation. Transects at the upstream end of the facility were eliminated first, then transects at the downstream end were eliminated. The length of the surf zone with the highest degree of longshore uniformity is defined as the length at which a minimum standard deviation is obtained.

Fig. 11 shows results for the regular wave experiment. Longshore variations in the average wave height measurements tend to decrease only slightly as the length of beach being considered is decreased. In contrast, longshore variations in the mean water surface elevation, and more importantly in the mean longshore current, decrease significantly with decreasing length of testing region, and approach a minimum asymptote at approximately 12 m. If a shorter length of surf zone is considered, there is no significant increase in uniformity. Therefore, it is concluded that the hydrodynamic measurements have reached a minimum longshore variability once the length of surf zone being considered is reduced to 12 m, starting at Y19 and extending upstream to Y31.

The high degree of longshore uniformity in this portion of the surf zone is illustrated in Fig. 12a–c, which shows the cross-shore distributions of measured wave height, mean water surface elevation, and mean longshore current, respectively, for transects Y19 through Y31. Fig. 12a shows that the greatest longshore variation in the measured wave height occurred at and immediately offshore of the incipient breaker line. Wave breaking occurred immediately shoreward of Wave Gauge 6. Deviations from the longshore averaged wave height were as large as $\pm 8\%$. This is a laboratory effect caused by generating regular waves in a wave basin with reflective boundaries. However, the longshore variation in wave height measured in front of each of the four generators ($x = 18$ m), had a standard deviation of only 2.8%. In the inner surf zone, the longshore uniformity in wave height is very good due to the dominant effect of depth, which limits wave height. The longshore averaged breaker height index, across the width of the surf zone (Wave Gauge 1 through 6), is calculated to be 0.74, and is tabulated in Table A-3 of Appendix A, with several other parameters.

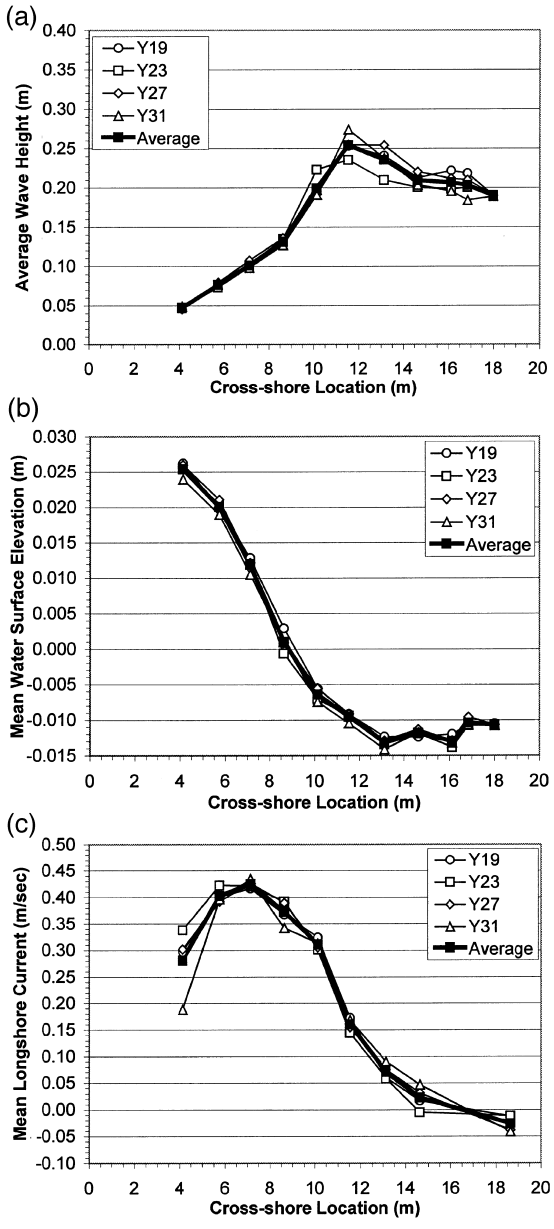

Fig. 12. (a) Test 6N: distribution of regular wave height. (b) Test 6N: distribution of mean water surface elevation. (c) Test 6N: distribution of mean longshore current.

Fig. 12b shows that the longshore variation in mean water surface elevation is approximately ± 0.0015 m. This value is comparable to the elevation tolerance of the bridge support rails. Therefore, it can be concluded that there is no measurable longshore gradient in the mean water level in this region. Fig. 12c shows that the degree of uniformity in the mean longshore current is quite good. The reduction in magnitude of the longshore current at $x = 4.1$ m at transect Y31 is caused by the small flow reversal region further upstream, close to the shoreline. It is interesting to note that just offshore of the peak longshore current, the measurements suggest a slight flattening of the longshore current distribution. This observation is qualitatively consistent with the present understanding of the interaction of the undertow with the longshore current, see Putrevu and Svendsen (1992).

Fig. 13 quantifies longshore uniformity of the hydrodynamic processes in the irregular wave experiment. As was found for the regular wave case, all three hydrodynamic parameters tend to approach a minimum asymptote, once the length of the testing region is reduced to approximately 12 m, starting at Y19 and extending upstream to Y31. The values of the standard deviation in the irregular wave experiment are significantly less than in the regular wave experiment, especially for the wave and current data. Perhaps the regular wave forcing generates a basin response that does not occur when using irregular wave forcing.

Fig. 14a–c illustrates the high degree of longshore hydrodynamic uniformity for the irregular wave case. Fig. 14a shows that the significant wave height is very uniform in the alongshore direction. The signifi-

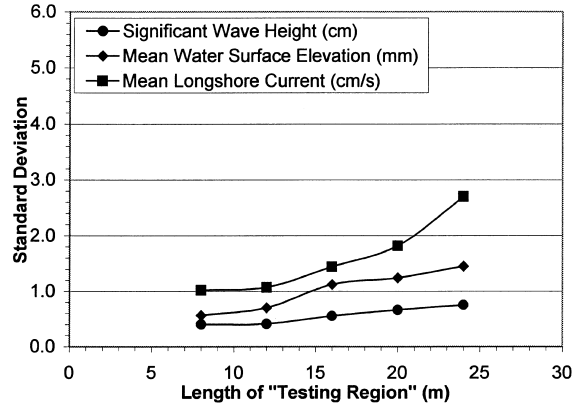

Fig. 13. Test 8E: longshore uniformity of hydrodynamics.

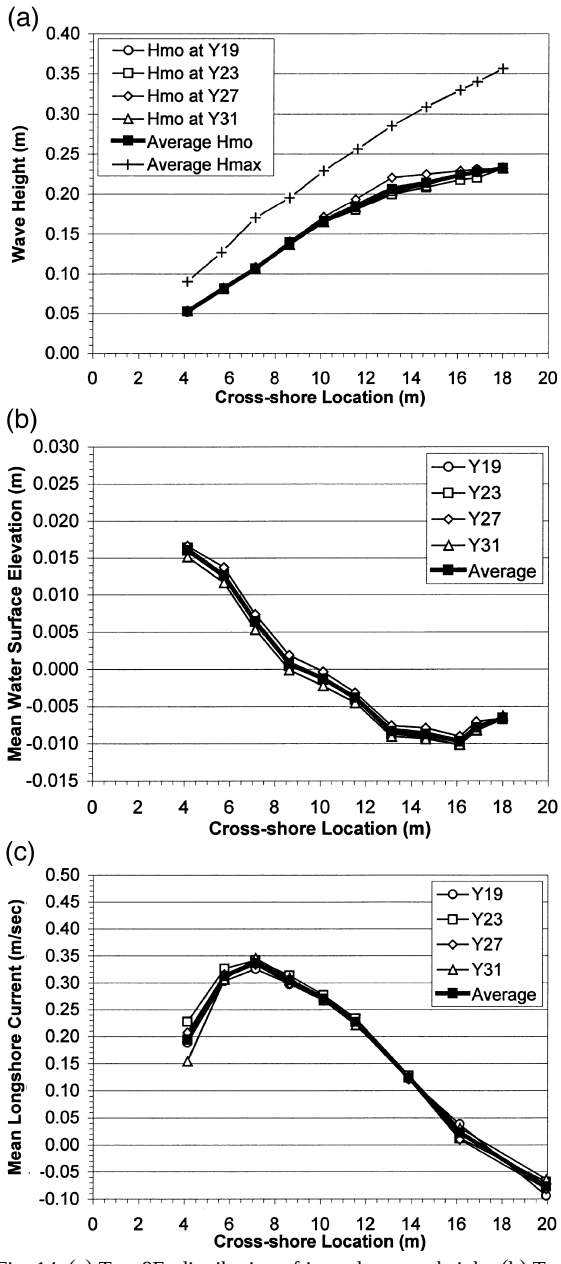

Fig. 14. (a) Test 8E: distribution of irregular wave height. (b) Test 8E: distribution of mean water surface elevation. (c) Test 8E: distribution of mean longshore current.

cant wave height at incipient breaking occurred immediately shoreward of Wave Gauge 7, based on visual observations and the fact that the gradient in the significant wave height curve increases significantly at that location. The longshore averaged breaker height index, across the width of the surf zone (Wave Gauge 1 through 7) is calculated to be 0.75, as tabulated in Table A-3 of Appendix A. The longshore averaged value of the measured maximum wave height is also shown to illustrate that $H_{max} > 0.35$ m at $x = 18$ m. As was the case for the regular wave test, Fig. 14b shows that the alongshore variation in mean water surface elevation is approximately ± 0.0015 m. The wave setup at $x = 4.1$ m is only about 60% of the value measured in the regular wave case, even though the incident wave energy was held constant by setting H_{rms} in the irregular wave case equal to H_{reg} in the regular wave case. Fig. 14c shows that the mean longshore current is very uniform in the longshore direction. The peak current is 0.34 m/s, relative to a peak current of 0.42 m/s in the regular wave case. The cross-shore distribution is broader than in the regular wave case, with the offshore tail decreasing much more uniformly. Dye was used to investigate the longshore current in very shallow water. No local increase in longshore current was detected shoreward of ADV 1 for either the regular or irregular wave case. It is interesting to note that the total longshore flow rate actively pumped through the lateral boundaries, Q_p is 465 and 478 l/s for the regular and irregular wave cases, respectively. These values are very similar, since the incident wave energy was held constant for the two cases, as mentioned previously.

The measured cross-shore distribution of the mean longshore current at transects Y19 through Y31, and the longshore-averaged values of the mean longshore current for these four transects, are provided in Appendix A. The longshore averaged values of wave height and mean water surface elevation, from Y19 through Y31, are also provided.

8. Longshore current steadiness and measurement repeatability

Individual fixed-bed hydrodynamic experiments lasted from 2 to 3 h, depending on the number of transects measured. The plan for moveable-bed longshore sediment transport experiments is to also operate the facility continuously for a several-hour duration, perhaps longer. Therefore, the issues of current

steadiness and repeatability over this time scale are important. Experiments were conducted to investigate the time required for the mean currents in the wave basin to reach steady-state conditions. Results from Test 8E, the irregular wave case, are shown in Fig. 15. The data represent the mean longshore current distribution measured at transect Y27 at three different times: 20, 110, and 150 min after the start of the experiment. Pumps were started at time zero. Wave generation commenced at the 10-min mark, after all 20 pumps had been adjusted to within 1% of the target discharge rates. Results showed that mean currents reached steady state within 10 min of starting the wave generators. The standard deviation of the mean longshore current, averaged for all cross-shore positions along Y27, was 0.0022 and 0.0017 m/s for Tests 8E and 6N, respectively.

A related issue is measurement repeatability. Current measurements at Y27 were repeated five times during Test 6N, one immediately after the other, to quantify the repeatability of the mean longshore current measurements. Each set of measurements was sampled for 500 s. The standard deviation of the five mean longshore current measurements, averaged for all cross-shore positions, was 0.0015 m/s. This confirmed that the repeatability of ADV measurements was quite good.

The steadiness of the current regime and the repeatability of the ADV measurements allowed the vertical mean current structure to be measured with a high degree of confidence. Measurements were made by accurately repositioning all of the ADV sensors at a new elevation in the water column, prior to each subsequent set of measurements. The vertical structure of the mean longshore current for Tests 6N and 8E are given in Appendix B.

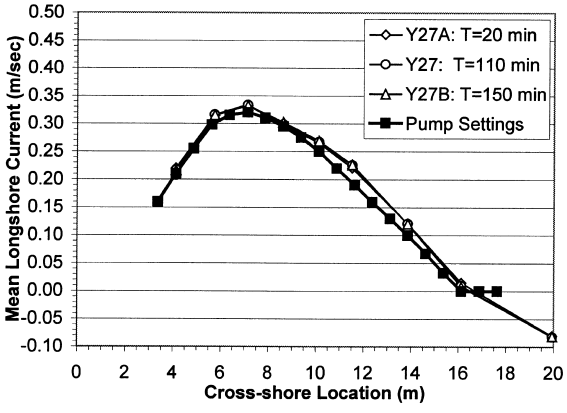

Fig. 15. Test 8E: sequential measurements of mean longshore current at Y27.

9. Application to sediment transport studies

As discussed in the previous section, the mean currents in the wave basin were found to reach steady state within 10 min of starting the wave generators. In addition, with experience, only approximately five iterations are required to converge on the proper pump settings. These are two very positive conclusions with respect to future sediment transport experiments in the LSTF, since the time will be minimized during which sediment will be moving in response to improper longshore currents.

As shown, the high cross-shore resolution of the longshore current recirculation system in the LSTF allows very accurate control of the longshore current distribution. Since the pumps are digitally controlled, and the in-line flow sensors allow for real-time data collection, it typically only takes 30–60 min to re-adjust the pump settings for a new iteration. Therefore, in future sediment transport experiments, the pump settings can be easily adjusted in response to changing beach morphology.

Most of the longshore sediment transport experiments will be conducted using irregular waves. For the irregular wave case, the degree of longshore uniformity in mean longshore current and wave height is quite good downstream to Y14, the closest transect to the downstream boundary. As shown in Fig. 16, there were small decreases in longshore current speed near the downstream boundary, on the order of 10% at the peak, relative to the average current for the 12-m region of the beach with the highest degree of longshore uniformity (Y19 through Y31). The reasonably high degree of longshore uniformity at the downstream end of the beach is a very positive result from the standpoint of conducting longshore sediment transport experiments in the LSTF, since the sand traps will be located at the downstream end of the beach. Nonetheless, some inefficiency is expected at the sand traps due to the slight reduction in current magnitude and wave energy at the downstream boundary.

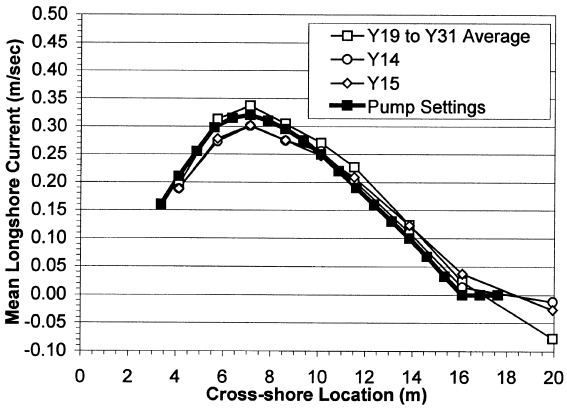

Fig. 16. Test 8E: distribution of mean longshore current at downstream boundary.

Finally, the large geometric scale of the wave conditions tested in the LSTF will generate a significant amount of suspended sediment transport. It is therefore necessary to maintain relatively straight and parallel current streamlines at the downstream boundary, so that the cross-shore distribution of the total longshore sediment transport rate, measured at the downstream boundary, is not skewed. For this reason, the external recirculation system was developed with the capability of controlling the cross-shore distribution of longshore current at both the upstream and downstream lateral boundaries.

10. Conclusions

Two comprehensive test series were conducted on an idealized concrete beach with straight and parallel contours, one involving regular waves and the other irregular waves. Both test series were conducted with long-crested, unidirectional waves. These data are valuable for several reasons: (1) the geometric scale of the experiments is significantly larger than the scale of laboratory experiments conducted in the past, (2) the concrete beach has a relatively mild 1:30 slope, unlike previous laboratory experiments, (3) both regular and irregular wave forcing were used, and (4) the vertical velocity structure of the longshore current was accurately measured using acoustic-doppler velocitimeters. The data are provided for use in theoretical studies and for calibration and verification of analytical and numerical models.

The pump settings that produced the proper longshore current distribution in the LSTF were determined through an iterative process based on mean longshore current measurements in the surf zone and offshore in the internal recirculation zone. This procedure was found to work well. When the proper distribution is pumped, the degree of longshore uniformity in mean longshore current increases noticeably, and the magnitude of the current offshore in the recirculation zone approaches a minimum value. Internal recirculation cannot be eliminated, however, and its magnitude was found to be about 10% of the total flow rate in the surf zone for the two wave cases examined.

The final selection of proper pump settings were confirmed by the insightful criteria developed by Visser (1991). But unlike the findings of Visser for the facility he used, for the LSTF, Q_p can vary by as much as $\pm 20\%$ of Q_{pu} without a significant increase in Q_r. For this reason, emphasis during the iterative process is placed on examination of the measured data, taking advantage of the high degree of cross-shore resolution in the recirculation system itself. However, even for this range of Q_p the inshore two-thirds of the mean longshore current distribution was relatively unaffected by Q_r. The effect of internal recirculation, Q_r manifested itself primarily on the offshore tail of the measured longshore current distribution. Therefore, the tuning focussed on the inshore portion of the distribution first, saving the offshore tail for last. Measured currents in the offshore tail were always higher than the equivalent pump settings, regardless of the magnitude.

The active external longshore current recirculation system and the operational procedure used to pump the proper current, led to a 12-m long region of the beach that was characterized by a very high degree of longshore uniformity in waves, currents, and mean water levels, between Y (longshore) coordinates of 19 and 31 m. Furthermore, as discussed in a previous section, the standard deviation of the longshore variation in longshore current is still relatively small downstream to $Y = 14$ m.

The steadiness of mean flow conditions, quality of the sensors, and repeatability of the measurements allow accurate data sets to be acquired, not only of

wave, current (at one depth), and water elevation parameters, but also the vertical structure of the mean current field. The steadiness and repeatability should allow high quality data sets of suspended sand concentrations and longshore sediment transport rates to be acquired during sediment transport experiments in the LSTF.

Acknowledgements

The authors would like to thank Dr. Richard Whitehouse for openly sharing his experience in developing the Coastal Research Facility at HR Wallingford, in the United Kingdom. Appreciation is also given to Dr. Paul Visser for meeting with the first author to discuss the experimental methodology used in his previous experiments, at Delft University of Technology, in The Netherlands. The research presented here was funded by the "Large-Scale Laboratory Investigation of Longshore Sediment Transport" work unit of the Coastal Sedimentation and Dredging Program of the General Investigations Research and Development Program of the U.S. Army Engineers. The internal reviews of Ms. Julie Rosati and Dr. Jane Smith and the valuable comments of Dr. J.W. Kamphuis and the anonymous reviewer are greatly appreciated. Permission to publish this paper was granted by the Office of the Chief of Engineers, U.S. Army Corps of Engineers.

Appendix A. Tabular data for the regular and irregular wave cases

The primary data sets for Tests 6N (regular waves) and 8E (irregular waves) are provided in tabular form in Tables A-1 and A-2, respectively. Each table lists the measured mean longshore current at transects Y19, Y23, Y27 and Y31 as well as the longshore-averaged value for these four transects, V_{avg}; the still water depth, d; the longshore-averaged value of wave set-up or set-down, η_{avg}, and wave height, H_{avg}. The energy-based significant wave height, listed for Test 8E, is based on using a lower cut-off frequency of 0.2 Hz (i.e., $0.5 \times F_p$), to remove the low frequency energy from the water surface elevation time series. The cross-shore (x-axis) positions of the measurements are listed in the standard basin coordinates (see Section 3 for a definition). The still water depth can be calculated as:

$$d = x/30 - 0.1, \quad \text{for} \quad 3.0\,\text{m} \le x \le 18.0\,\text{m} \qquad \text{(A-1)}$$

$$d = x/18 - 0.5, \quad \text{for} \quad 18.0\,\text{m} \le x \le 21.0\,\text{m} \qquad \text{(A-2)}$$

$$d = 0.667\,\text{m}, \quad \text{for} \quad x \ge 21.0\,\text{m} \qquad \text{(A-3)}$$

Table A-3 provides a number of other measured and calculated wave and water level quantities in the surf zone, where h is the longshore-averaged mean water depth (equal to $d + \eta$), η is the mean water surface elevation, η_m is the maximum value of wave set-up, estimated by linear extrapolation, γ is the

Table A-1
Primary data set from regular wave Test 6N

X-Loc. (m)	Y19 (m/s)	Y23 (m/s)	Y27 (m/s)	Y31 (m/s)	V_{avg} (m/s)	d (m)	η_{avg} (m)	H_{avg} (m)
4.12	0.297	0.338	0.302	0.188	0.281	0.037	0.025	0.047
5.72	0.401	0.422	0.392	0.397	0.403	0.091	0.020	0.077
7.12	0.417	0.421	0.426	0.434	0.424	0.137	0.012	0.101
8.62	0.368	0.392	0.390	0.342	0.373	0.187	0.001	0.131
10.12	0.323	0.301	0.305	0.312	0.310	0.237	−0.006	0.199
11.52	0.173	0.145	0.154	0.169	0.160	0.284	−0.010	0.254
13.12	0.060	0.058	0.075	0.090	0.071	0.337	−0.013	0.235
14.62	0.016	−0.005	0.031	0.046	0.022	0.387	−0.012	0.209
15.62	–	–	−0.007	–	−0.007	0.421	–	–
16.12	–	–	–	–	–	0.437	−0.013	0.206
16.85	–	–	–	–	–	0.462	−0.010	0.203
18.00	–	–	–	–	–	0.500	−0.011	0.190

Table A-2
Primary data set from irregular wave Test 8E

X-Loc. (m)	Y19 (m/s)	Y23 (m/s)	Y27 (m/s)	Y31 (m/s)	V_{avg} (m/s)	d (m)	η_{avg} (m)	$H_{mo\text{-}avg}$ (m)
4.12	0.188	0.227	0.207	0.154	0.194	0.037	0.016	0.053
5.72	0.303	0.326	0.316	0.306	0.313	0.091	0.013	0.082
7.12	0.326	0.341	0.333	0.346	0.337	0.137	0.006	0.107
8.62	0.297	0.313	0.298	0.309	0.304	0.187	0.001	0.138
10.12	0.270	0.277	0.267	0.267	0.270	0.237	−0.001	0.167
11.52	0.228	0.233	0.226	0.221	0.227	0.284	−0.004	0.185
13.12	–	–	–	–	–	0.337	−0.008	0.206
13.88	0.122	0.128	0.121	0.125	0.124	0.363	–	–
14.62	–	–	–	–	–	0.387	−0.009	0.214
16.12	0.038	0.012	0.010	0.031	0.023	0.437	−0.010	0.224
16.85	–	–	–	–	–	0.462	−0.008	0.227
18.00	–	–	–	–	–	0.500	−0.007	0.232

Table A-3
Summary of wave and water level conditions in the surf zone

Test	H_{br} (m)	h_{br} (m)	H_{br}/h_{br} (–)	γ (–)	θ_{br} (°)	X_{br} (m)	η_m (m)	X-Loc. at η_m (m)	X-Loc. at SWL (m)
Test 6N	0.254	0.274	0.93	0.74	6.7	11.5	0.033	2.1	3.00
Test 8E	0.206	0.329	0.63	0.75	7.3	13.1	0.021	2.4	3.00

surf zone averaged value of H/h, and the subscript, "br", refers to values at the breaker line. The breaking wave angle, θ_{br}, was estimated using Snell's law.

For the regular wave case, the breaking point is assumed to be the point where the measured wave height reaches its maximum value. For the irregular wave case, the breaking point was assumed to be the

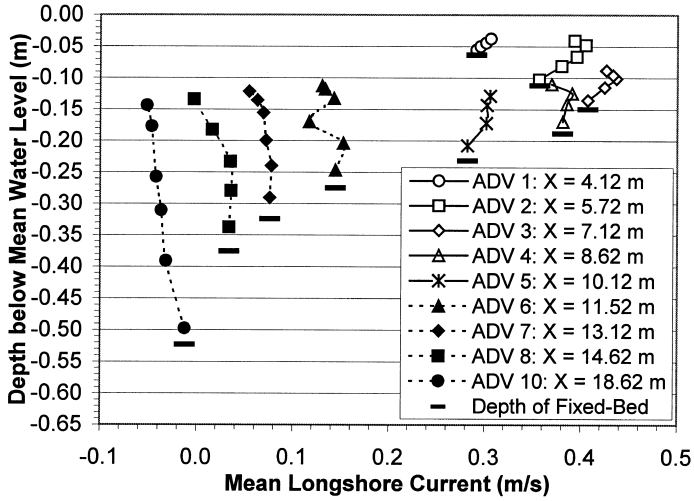

Fig. B1. Regular wave Test 6N: vertical structure of the mean longshore current at Y27.

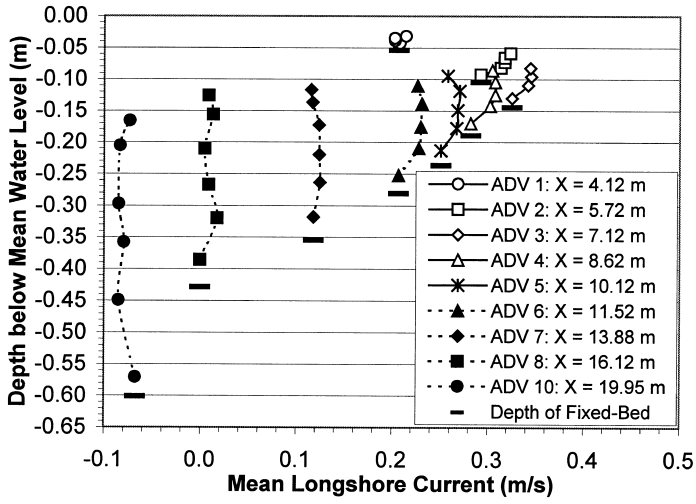

Fig. B2. Irregular wave Test 8E: vertical structure of the mean longshore current at Y27.

point where the measured significant wave height began to decrease at the highest rate (see Fig. 14a). This occurred at the location $x = 13.1$ m, where the longshore-averaged significant wave height was 0.21 m.

Estimates of the position of the mean water line are $x = 2.1$ m for the regular wave case and $x = 2.4$ m for the irregular wave case. It should be noted that the cross-shore position of the mean water line could only be estimated with an accuracy of approximately ± 0.1 m. Therefore, the estimates of maximum wave set-up are only accurate within ± 0.003 m.

Appendix B. Vertical structure of the mean longshore current

Fig. B1 shows the cross-shore variation in the vertical structure of the mean longshore current for the regular wave case (Test 6N). In general, the mean longshore current is rather uniform with depth. In the inner surf zone (ADV 1 through 5), there is a slight increase in current speed with distance from the bed, and outside the surf zone (ADV 7 and 8) a slight decrease in current speed with distance from the bed. Visser (1991) measured similar trends in the vertical velocity structure using regular waves. Putrevu and Svendsen (1992) presented a theoretical model that predicts similar trends in the vertical velocity structure. ADV 6 was located at the position of incipient wave breaking.

Fig. B2 shows the vertical structure of the mean longshore current for the irregular wave case (Test 8E). The mean longshore current in this case is also rather uniform with depth. In the inner surf zone (ADV 1 through 6), there is a slight increase in current speed with distance from the bed, and the vertical variations are similar to those measured for the regular wave case. In the outer surf zone (ADV 7 and 8), the mean velocity is relatively invariant with depth. This trend is different from that in the regular wave case, where the mean velocity decreased slightly with increasing distance from the bottom. However, in the regular wave case, no waves were breaking at ADV 7 and 8; whereas in the irregular wave case, some wave breaking occurred in this region.

References

Brebner, A., Kamphuis, J.W., 1963. Model tests on the relationship between deep-water wave characteristics and longshore currents. Civil Eng. Res. Rep. 31, Queen's University, Kingston, Ontario, Canada, 28 pp.

Dalrymple, R.A., Dean, R.G., 1972. The spiral wavemaker for littoral drift studies. Proc. 13th Int. Conf. Coastal Eng., Vancouver, Canada. pp. 689–705.

Dalrymple, R.A., Eubanks, R.A., Birkemeier, W.A., 1977. Wave-induced circulation in shallow basins. J. Waterway, Port, Coastal Ocean Div. 103, 117–135.

Galvin, C.J., Eagleson, P.S., 1965. Experimental study of longshore currents on a plane beach. U.S. Army Coastal Eng. Research Center, Vicksburg, Mississippi, Tech. Memo. No. 10, 80 pp.

Hamilton, D.G., Smith, E.R., Ebersole, B.A., Wang, P., 2000. Development of a large-scale laboratory facility for sediment transport research. U.S. Army Engineer Research and Development Center, Coastal and Hydraulic Laboratory, Vicksburg, MS, Tech. Report, Vol. I (in preparation).

Hamilton, D.G., Rosati, J.D., Fowler, J.E., Smith, J.M., 1996. Design capacity of a longshore current recirculation system for a longshore sediment transport laboratory facility. Proc. 25th Int. Conf. Coastal Eng., Orlando, FL, ASCE. pp. 3628–3641.

Hamilton, D.G., Neilans, P.J., Rosati, J.D., Fowler, J.E., Smith, J.M., 1997. Hydraulic design of a large-scale longshore current recirculation system. Proc. Coastal Dynamics '97, Plymouth, United Kingdom, ASCE. pp. 516–525.

HR Wallingford, 1994. Understanding the nearshore environment. Publication describing the Coastal Research Facility at HR Wallingford, Wallingford, England, 4 pp.

Kamphuis, J.W., 1977. Discussion on wave-induced circulation in shallow basins. J. Waterway, Port, Coastal Ocean Div. 103, 570–571.

Kraus, N.C., Larson, M., 1991. NMLONG: Numerical model for simulating the longshore current, Report 1: Model development and tests. U.S. Army Coastal Eng. Research Center, Tech. Report DRP-91-1, Vicksburg, Mississippi, 143 pp.

Mizuguchi, M., Horikawa, K., 1978. Experimental study on longshore current velocity distribution. Fac. Sci. Eng. 21, 123–150, Chuo Univ., Tokyo, Japan, Bull.

Putnam, J.A., Munk, W.H., Traylor, M.A., 1949. The prediction of longshore currents. Trans. Am. Geophys. Union 30, 337–345.

Putrevu, U., Svendsen, I.A., 1992. A mixing mechanism in the nearshore region. Proc. 23rd Int. Conf. Coastal Eng, Venice, Italy, ASCE. pp. 2758–2771.

Putrevu, U., Oltman-Shay, J., Svendsen, I.A., 1995. Effects of alongshore nonuniformities on longshore current predictions. J. Geophys. Res. 100, 16119–16130.

Reniers, A.J.H.M., Battjes, J.A., 1997. A laboratory study of longshore currents over barred and non-barred beaches. Coastal Eng. 30, 1–22.

Rosati, J.D., Hamilton, D.G., Fowler, J.E., Smith, J.M., 1995. Design of a laboratory facility for longshore sediment transport research. Proc. Coastal Dynamic '95, Gdansk, Poland, ASCE. pp. 771–782.

Simons, R.R., Whitehouse, R.J.S., MacIver, R.D., Pearson, J., Sayers, P.B., Zhao, Y., Channell, A.R., 1995. Evaluation of the UK Coastal Research Facility. Proc. Coastal Dynamics '95, Gdansk, Poland, ASCE. pp. 161–172.

Svendsen, I.A.,1991. Development of a comprehensive plan for modeling longshore current generation in the laboratory. Unpublished Report for the U.S. Army Coastal Eng. Research Center, Vicksburg, Mississippi, 56 pp.

Visser, P.J., 1980. Longshore current flows in a wave basin. Proc. 17th Int. Conf. Coastal Eng., Sydney, ASCE. pp. 462–479.

Visser, P.J.,1982. The proper longshore current in a wave basin. Comm. on Hyd. Rep. 82-1, Dept. of Civil Eng. Delft Univ. of Technology, Delft, The Netherlands, 86 pp.

Visser, P.J., 1984. Uniform longshore current measurements and calculations. Proc. 19th Int. Conf. Coastal Eng., Houston, ASCE, 2192–2207.

Visser, P.J., 1991. Laboratory measurements of uniform longshore currents. Coastal Eng. 15, 563–593.